The Sjögren-Larsson Syndrome Gene Encodes a Hexadecenal Dehydrogenase of the Sphingosine 1-Phosphate Degradation Pathway

Kanae Nakahara,[1,3] Aya Ohkuni,[1,3] Takuya Kitamura,[1] Kensuke Abe,[1] Tatsuro Naganuma,[1] Yusuke Ohno,[1] Raphael A. Zoeller,[2] and Akio Kihara[1,*]

[1]Laboratory of Biochemistry, Faculty of Pharmaceutical Sciences, Hokkaido University, Kita 12-jo, Nishi 6-chome, Kita-ku, Sapporo 060-0812, Japan

[2]Department of Physiology and Biophysics, Boston University School of Medicine, 700 Albany St., W-317, Boston, MA 02118-2526

[3]These authors contributed equally to this work.

[*]Correspondence:

Akio Kihara

Laboratory of Biochemistry, Faculty of Pharmaceutical Sciences, Hokkaido University

Kita 12-jo, Nishi 6-chome, Kita-ku, Sapporo 060-0812, Japan

Tel: +81-11-706-3754

Fax: +81-11-706-4900

E-mail: kihara@pharm.hokudai.ac.jp

Running title: Hexadecenal Dehydrogenase in S1P Degradation

SUMMARY

Sphingosine 1-phosphate (S1P) functions not only as a bioactive lipid molecule but also as an important intermediate of the sole sphingolipid-to-glycerolipid metabolic pathway. However, the precise reactions and the enzymes involved in this pathway remain unresolved. We report here that yeast *HFD1* and the Sjögren-Larsson syndrome (SLS)-causative mammalian gene *ALDH3A2* catalyze conversion of the S1P degradation product hexadecenal to hexadecenoic acid. The absence of ALDH3A2 in CHO-K1 mutant cells caused abnormal metabolism of S1P/hexadecenal to ether-linked glycerolipids. Moreover, we demonstrate that yeast Faa1 and Faa4 and mammalian ACSL family members are acyl-CoA synthetases involved in the sphingolipid-to-glycerolipid metabolic pathway, and that hexadecenoic acid accumulates in Δ*faa1* Δ*faa4* mutant cells. These results unveil the entire S1P metabolic pathway: S1P is metabolized to glycerolipids via hexadecenal, hexadecenoic acid, hexadecenoyl-CoA, and palmitoyl-CoA. From our results we propose a possibility that accumulation of the S1P metabolite hexadecenal is contributed to the pathogenesis of SLS.

INTRODUCTION

Sphingosine 1-phosphate (S1P) plays important roles as an intracellular signaling molecule and as a ligand for G protein-coupled receptors ($S1P_1$ to $S1P_5$) (Kihara et al., 2007; Pyne and Pyne, 2011). The FDA-approved immunomodulator FTY720 undergoes *in vivo* phosphorylation then mimics S1P ligand functions (Pyne and Pyne, 2011). S1P also functions as an intermediate in the metabolism of sphingolipids (Kihara et al., 2007), which function in biological processes and are major components of eukaryotic plasma membranes (Kihara et al., 2007; Kolesnick and Krönke, 1998).

Sphingolipid metabolism involves salvage pathways that generate the sphingolipid backbone ceramide (Cer) and/or its component sphingosine (Sph), which are then utilized to rebuild sphingolipids. Alternatively, the Sph is phosphorylated by a Sph kinase to form S1P (Kihara et al., 2007). S1P can be metabolized to glycerolipids through degradation involving a S1P lyase, which cleaves S1P into a fatty aldehyde (hexadecenal) and phosphoethanolamine (Kihara et al., 2007) (Figure 1A). Disorders in sphingolipid metabolism, termed sphingolipidoses, are well known, with ~40 having been identified thus far (Sillence and Platt, 2003). However, to date, no such disorder has been associated with S1P or its metabolism. Beyond the generation of hexadecenal, no precise metabolic pathway has been determined for S1P-to-glycerolipid conversion, and little is understood regarding the enzymes involved or any disorders arising from their disruption. Considering that aldehyde molecules are highly reactive, for example with primary amines (James and Zoeller, 1997), it would be expected for aberrations in S1P metabolism to lead to pathological disorders.

Cer comprises a long-chain base (LCB) attached to fatty acid (FA) via an amide bond. Sph, the major LCB in mammals, contains a *trans*-double bond between C4 and C5, while another LCB, dihydrosphingosine (DHS), has no double bond (Figure 1A). DHS is generated via the *de novo* sphingolipid synthesis pathway and is metabolized similarly to S1P (Figure

1A). The metabolic pathway of DHS1P has already been identified (Kihara et al., 2007) (Figure 1A), yet it is unknown when and how the *trans*-double bond derived from S1P is converted to the saturated bond. Moreover, the fatty aldehyde dehydrogenase (FALDH), the acyl-CoA synthetase (ACS), and the saturating enzyme involved in S1P/DHS1P metabolic pathway all remain unidentified.

ALDH3A2 is an FALDH that exhibits activity toward saturated and unsaturated aliphatic aldehydes of 6 to 24 carbons in length (Kelson et al., 1997). Mutations in the *ALDH3A2* gene cause Sjögren-Larsson syndrome (SLS), the neurocutaneous disorder characterized by congenital ichthyosis, mental retardation, and spasticity (De Laurenzi et al., 1996; Rizzo, 2007). Although accumulated fatty aldehydes in SLS patients are thought to be responsible for the pathology, the source of the accumulation remains unclear. In the presented study, we have identified ALDH3A2 as the FALDH active within the S1P metabolic pathway.

ACSs catalyze the conversion of FAs to their activated forms, *i.e.*, acyl-CoAs. The yeast *Saccharomyces cerevisiae* and mammals have 7 and 26 ACSs, respectively (Black and DiRusso, 2007; Watkins et al., 2007). In the presented study, we identified Faa1 and Faa4 in yeast and ACSL1, ACSL3, ACSL4, ACSL5, and ACSL6 in mammals as ACSs responsible for S1P/DHS1P metabolic pathways. We also demonstrated that hexadecenoic acid is the intermediate of S1P metabolism. From these results, we determined the entire S1P metabolic pathway.

RESULTS

Yeast Hfd1 and Mammalian ALDH3A2 Are Involved in LCB/LCB 1-Phosphate Metabolism

Metabolism of LCBs/LCB 1-phosphates (LCBPs) and the enzymes responsible are mostly conserved from yeast to man. Therefore, we first used the yeast *S. cerevisiae* for identification of the FALDH involved in the metabolism of LCBs/LCBPs. Wild type yeast cells and 8 yeast strains carrying mutations in genes encoding aldehyde dehydrogenases (Δ*hfd1*, Δ*ald2*, Δ*ald3*, Δ*ald4*, Δ*ald5*, Δ*ald6*, Δ*uga2*, and Δ*msc7*), as well as a mutant for the LCBP lyase gene (Δ*dpl1*) (as a control) were labeled with [4,5-^{3}H]DHS. In wild type cells DHS was metabolized to both sphingolipids (Cer, inositol phosphorylceramide (IPC), mannosylinositol phosphorylceramide (MIPC), and mannosyldiinositol phosphorylceramide ($M(IP)_2C$)) and glycerolipids (phosphatidylethanolamine (PE), phosphatidylcholine (PC), phosphatidylserine (PS), and phosphatidylinositol (PI)) (Figure 2A and Figure S1A). In contrast, DHS was not converted to glycerolipids in the Δ*dpl1* cells (Figure 2A), as expected from its function in the LCB/LCBP metabolic pathway (Figure 1B).

Of the 8 aldehyde dehydrogenase mutants, only the Δ*hfd1* cells exhibited a deficiency in DHS-to-glycerolipid conversion (Figure 2A), indicating that Hfd1 is the FALDH involved in the metabolism of DHS/DHS1P in yeast. In the Δ*hfd1* cells, hexadecanol but not hexadecanal accumulated (Figure S1B), suggesting that the some unmetabolized hexadecanal was reduced to hexadecanol. However, the accumulated hexadecanol levels were lower than would be expected when considering the sum of glycerolipid levels in wild type cells (Figure 2A and Figure S1A and B). We speculate that most of the unmetabolized hexadecanal might have reacted with several cellular components having primary amines before being converted to hexadecanol.

To date, no function for Hfd1 has been identified. Homology searches revealed that,

among mammalian aldehyde dehydrogenases, Hfd1 shares the highest sequence similarity with mammalian ALDH3A2 (30.0% identity and 50.6% similarity). The *ALDH3A2* gene is known to be responsible for the neurocutaneous disorder SLS (Rizzo, 2007). ALDH3A2 reportedly exhibits activity toward saturated and unsaturated aliphatic aldehydes ranging from 6 to 24 carbons in length (Kelson et al., 1997). To establish that ALDH3A2 is involved in the DHS/DHS1P metabolism, we introduced the human *ALDH3A2* gene into the Δ*hfd1* yeast cells, and examined the metabolism of [4,5-^{3}H]DHS. Introduction of the *ALDH3A2* gene resulted in the recovery of DHS conversion to glycerolipids in cells deficient in Δ*hfd1* (Figure 2B), indicating that ALDH3A2 and Hfd1 are functional homologs and are involved in DHS/DHS1P metabolism.

Generation of [11,12-^{3}H]Sph and Its Metabolism in Yeast and in Mammalian Cells

A lack of radiolabeled S1P or Sph for use as tracers has hampered study into their metabolic pathway. Commercially available [3-^{3}H]Sph can label sphingolipids but not glycerolipids, since the 3-^{3}H atom is removed during S1P conversion to hexadecenal by S1P lyase (Figure S2A and B). In contrast, 4,5-^{3}H labeled DHS enables monitoring of its metabolism both to sphingolipids and to glycerolipids (Figure S2A and B). In a late 1960s study, [7-^{3}H]Sph administered intravenously to a rat was converted in the liver to both sphingolipids and glycerolipids, and the major Sph-derived FA in glycerolipids was palmitic acid (Stoffel and Sticht, 1967). No further analysis of Sph-to-glycerolipid metabolism has been performed, leaving a gap in our knowledge of this important metabolic pathway. To address this deficit, we prepared traceable [11,12-^{3}H]Sph from [9,10-^{3}H]palmitic acid. When [11,12-^{3}H]Sph was separated by TLC with commercially available [3-^{3}H]Sph and [4,5-^{3}H]DHS, [11,12-^{3}H]Sph presented as a single band that migrated at the position identical to [3-^{3}H]Sph (Figure 3A). When incubated with Sph kinase, [11,12-^{3}H]Sph was completely converted to S1P (Figure 3B).

These results indicate that our [11,12-^{3}H]Sph is highly pure.

To date, Sph-to-glycerolipid metabolism has not been examined using mammalian cultured cells, so it remains unclear whether Sph is converted to glycerolipids as efficiently as DHS. To test this, human embryonic kidney (HEK) 293T cells were labeled with [4,5-^{3}H]DHS or [11,12-^{3}H]Sph. DHS and Sph were metabolized to sphingolipids and to glycerolipids with similar efficiency (Figure 3C). In this experiment, half of the samples were treated with alkaline solution. Since ester linkages in glycerolipids are hydrolyzed by alkaline treatment, glycerolipid bands disappeared, while sphingolipid bands remained unchanged (Figure 3C). Using another cell line, mouse embryonic carcinoma F9 cells, we repeated the labeling experiments. We also used F9 *SPL*$^{-/-}$ cells, which lack the S1P lyase SPL, as a negative control that cannot convert DHS or Sph to glycerolipids (Ikeda et al., 2005). Again, Sph and DHS were similarly metabolized to sphingolipids and to glycerolipids in wild type F9 cells, but were metabolized only to sphingolipids in the *SPL*$^{-/-}$ cells (Figure 3D). Cer and glucosylceramide (GlcCer), observed at high levels after a 2 hr labeling period, had decreased by 24 hr. Instead, lactosylceramide (LacCer), which is a further metabolite of GlcCer, and the glycerolipids PE and PS/PI had increased. These results indicate that DHS and Sph are similarly metabolized in mammalian cells.

Natural LCBs found in the yeast *S. cerevisiae* include DHS and phytosphingosine (Figure 1B). Sph is not found in the yeast, yet the yeast can still use exogenously added Sph as a precursor for sphingolipids (Tani et al., 2006). We labeled yeast cells with [11,12-^{3}H]Sph and examined its metabolism and compared it with that of labeled DHS. In contrast to their conversion in mammalian cells, DHS and Sph were not metabolized similarly in wild type yeast cells. DHS was metabolized efficiently to sphingolipids and glycerolipids, whereas Sph was converted mainly to glycerolipids, with a small amount converted to sphingolipids (Figure 4A); it is possible that sphingolipid biosynthetic enzymes such as Cer synthase might have

lower activities toward Sph. Again, the DHS-to-glycerolipid conversion was Dpl1- and Hfd1-dependent (Figure 4A). This Sph-to-glycerolipid metabolic pathway was blocked in Δ*hfd1* cells as in Δ*dpl1* cells (Figure 4A), indicating that Hfd1 catalyzes not only conversion of hexadecanal derived from DHS1P to palmitic acid, but also that of hexadecenal (more precisely *trans*-2-hexadecenal) from S1P to hexadecenoic acid (*trans*-2-hexadecenoic acid). We also observed accumulation of hexadecenol in the Δ*hfd1* cells (Figure S1B), which might reflect unmetabolized hexadecenal reduced to hexadecenol. Introduction of human *ALDH3A2* cDNA into the Δ*hfd1* cells restored the Sph-to-glycerolipid conversion (Figure 4B), similar to results in the [4,5-^{3}H]DHS labeling experiment (Figure 2B). To date, the enzymatic activity of ALDH3A2 toward *trans*-2-hexadecenal has not been investigated. However, our results suggest that ALDH3A2 is active toward 2-*trans*-hexadecenal. To confirm this, we performed *in vitro* assays using affinity-purified 3xFLAG-ALDH3A2. ALDH3A2 did indeed exhibit FALDH activities toward both 2-*trans*-hexadecenal and hexadecanal, although its activity toward hexadecanal was ~2 fold higher than that toward 2-*trans*-hexadecenal (Figure 4C).

Sph was proven to be metabolized to palmitic acid in glycerolipids in mammals (Stoffel and Sticht, 1967). However, it was unclear whether in yeast the FA in glycerolipids converted from Sph is also palmitic acid or if it is hexadecenoic acid still containing the 2-*trans* double bond. To examine the FA species in glycerolipids derived from Sph, lipids were extracted from wild type yeast cells labeled with [11,12-^{3}H]Sph, treated with alkaline solution to release FAs, and separated by TLC using hexane/diethylether/acetic acid (30:70:1, v/v), a resolving buffer that can separate palmitic acid and hexadecenoic acid. The FA derived from Sph migrated at a position identical to that of palmitic acid but not hexadecenoic acid (Figure 4D). Similarly, FA derived from [11,12-^{3}H]Sph in mammalian cells and FAs derived from [4,5-^{3}H]DHS in either yeast or mammalian cells all migrated at a position identical to that of palmitic acid but not hexadecenoic acid (Figure 4D). These results indicate that both Sph and DHS are converted to

palmitic acid irrespective of yeast and mammalian cells.

Molecular species of FA derived from Sph in yeast was also examined by double bond cleavage assay. Carbon to carbon double bonds can be cleaved with KIO_4 in the presence of $KMnO_4$ (Scarim et al., 1989). This method can determine whether FA derived from Sph in yeast is saturated palmitic acid or unsaturated hexadecenoic acid. Control palmitic acid was indeed resistant to KIO_4/$KMnO_4$ treatment, whereas hexadecenoic acid was sensitive (Figure 4E). Both the FAs metabolized from [11,12-^{3}H]Sph in either HEK 293T cells or yeast were resistant to KIO_4/$KMnO_4$ treatment, confirming the above results that FA in glycerolipids converted from Sph is palmitic acid both in yeast and in mammals. Taken together, these results affirm that both Sph and DHS are converted to glycerolipids after conversion to palmitoyl-CoA. Thus, the Sph-to-glycerolipid metabolic pathway is highly conserved between yeast and mammals.

Aldehyde molecules are toxic to cells due to their high reactivity (James and Zoeller, 1997). We examined the toxicity of endogenously generated hexadecanal and hexadecenal by adding DHS or Sph to the medium of wild type, Δ*hfd1*, or Δ*dpl1* yeast cells. The Δ*hfd1* cells were more sensitive both to DHS and to Sph, as compared to wild type cells (Figure S3A and B). The Δ*dpl1* cells were also sensitive to DHS and Sph, but especially to Sph (Figure S3A). However, in the Δ*dpl1* cells toxicities were caused by an accumulation of LCBPs and the more toxic effect of Sph reflects higher accumulation levels of S1P compared to DHS1P in the Δ*dpl1* cells (Figure 4A) (Zhang et al., 2001). In the Δ*hfd1* cells, both S1P and DHS1P levels were similar to those in wild type cells (Figure 4A), so the sensitivity to exogenous LCBs observed for these cells may be caused by toxicities of endogenously generated fatty aldehydes.

LCBs/LCBPs are Metabolized to Ether-linked Glycerolipids in *ALDH3A2*-deficient

CHO-K1 Cells

We next investigated the involvement of ALDH3A2 in LCB/LCBP metabolism using mammalian cells. FAA-K1A cells were isolated from CHO-K1 cells as a FALDH mutant cell line; these cells displayed ~10% of the FALDH activity compared to CHO-K1 cells (James and Zoeller, 1997). RT-PCR revealed that *ALDH3A2* mRNA was barely detectable in the FAA-K1A cells (Figure 5A). CHO-K1 and FAA-K1A cells were labeled with [4,5-^{3}H]DHS, and lipids were separated by TLC. DHS was metabolized to both sphingolipids and glycerolipids in CHO-K1 cells (Figure 5B), similar to results in the HEK 293T and F9 cells described above (Figure 3C and D). In contrast, in FAA-K1A cells, the PC level was greatly reduced, but another lipid, which migrated adjacent to and slightly above PC, was produced (Figure 5B, arrowhead). This lipid was determined to be another type of choline glycerophospholipid, ether-linked glycerophospholipid (1-alkyl/alkenyl-2-acyl-glycero-3-phosphocholine), since it was not converted to FA but to 1-alkyl (or alkenyl)-glycerophosphocholine (GPC) by alkaline treatment (Figure 5B, dot), due to an alkaline-resistant ether bond. Little [4,5-^{3}H]DHS was converted to PS or PI in the FAA-K1A cells. PE was also reduced, but again ether-linked ethanolamine glycerophospholipid (1-alkyl/alkenyl-2-acyl-glycero-3-phosphoethanolamine) appeared in FAA-K1A cells (Figure 5B, arrowhead). In mammals, most ether-linked glycerophospholipids contain choline or ethanolamine as a polar group and can be divided into plasmanyl type glycerophospholipids (plasmanylcholine and plasmanylethanolamine) containing a 1-alkyl group, and plasmenyl type glycerophospholipids (plasmenylcholine and plasmenylethanolamine) containing a 1-alkenyl group. The plasmenyl type glycerophospholipids are also called plasmalogens, and these play a variety of cellular functions including functioning in membrane dynamics, acting as a source of arachidonic acid for generation of lipid mediators, intracellular signaling, and performing as antioxidants

(Nagan and Zoeller, 2001). To determine whether the observed ether-linked glycerophospholipids were plasmanyl or plasmenyl type, we treated the labeled lipids with acid. Plasmenyl glycerophospholipids (plasmalogens) are known to be sensitive to acid due to a reactive vinyl ether double bond (Nagan and Zoeller, 2001) (Figure S4A). The ether-linked choline glycerophospholipid was resistant to acid, whereas the ether-linked ethanolamine glycerophospholipid was sensitive (Figure 5B), indicating that they were plasmanylcholine and plasmenylethanolamine, respectively. Similar results were obtained when cells were labeled with [11,12-^{3}H]Sph (Figure 5B). In both labeling experiments, the band intensities of 1-alkyl-GPC and 1-alkenyl-glycerophosphoethanolamine (GPE) (Figure 5B, dots) were weaker than those of the original plasmanylcholine and plasmenylethanolamine (Figure 5B, arrowheads). This suggests that LCBs were metabolized both to the *sn*-1 alkyl/alkenyl groups and the *sn*-2 acyl group of the plasmanylcholine/plasmenylethanolamine. Our results suggest that fatty aldehyde derived from LCBs that had accumulated due to deficiency in ALDH3A2 was converted to fatty alcohol and utilized in the synthesis of ether-linked glycerolipids.

To confirm that ALDH3A2 is indeed responsible for the reduced ester-linked glycerolipid labeling and the generation of label in ether-linked glycerolipids in the FAA-K1A cells, we generated FAA-K1A cells stably expressing 3xFLAG-ALDH3A2. Two independent cell lines (FAA-ALDH3A2.A and FAA-ALDH3A2.B cells) expressed 3xFLAG-ALDH3A2 at similar levels (Figure S4B). A [4,5-^{3}H]DHS labeling experiment revealed that the plasmenylethanolamine and plasmanylcholine observed in FAA-K1A cells both disappeared in these stable clones, and PC and PS/PI levels were restored to the levels found in CHO-K1 cells (Figure S4C). Thus, a lack of ALDH3A2 causes metabolism of LCBs/LCBPs to ether-linked glycerolipids in CHO-K1 cells.

Hexadecenoic Acid is an Intermediate in the Sph/S1P Metabolic Pathway

FAs must be converted to acyl-CoAs prior to their incorporation into glycerolipids. However, the ACSs involved in LCB/LCBP metabolism have not been identified. Yeast have 7 ACSs (Faa1, Faa2, Faa3, Faa4, Fat1, Fat2, and Acs1). To identify which ACSs are involved in LCB/LCBP metabolism in yeast, a [4,5-^{3}H]DHS labeling experiment was performed using single deletion mutants or double deletion mutants of the yeast ACS genes. Of the mutants, only the Δ*faa1* Δ*faa4* double deletion mutant was defective in converting DHS to glycerolipids (Figure 6A), indicating that Faa1 and Faa4 function redundantly in the DHS/DHS1P metabolic pathway. When [11,12-^{3}H]Sph was used for labeling, abundant glycerolipids produced in wild type cells were greatly reduced in Δ*faa1* Δ*faa4* cells (Figure 6B), and instead, accumulation of FA, the substrate of the ACSs, was observed (Figure 6B, dot). Thus, Faa1 and Faa4 function not only in DHS/DHS1P metabolism but also in the Sph/S1P metabolic pathway in yeast. To identify the molecular species of the accumulated FA, the Δ*faa1* Δ*faa4* cells were labeled with [11,12-^{3}H]Sph, and lipids were separated by TLC using as a solvent system hexane/diethylether/acetic acid (30:70:1, v/v), which can separate palmitic acid and hexadecenoic acid. The FA accumulated in Δ*faa1* Δ*faa4* cells labeled with [11,12-^{3}H]Sph migrated to a position identical to that of hexadecenoic acid (Figure 6C) and was sensitive to KIO_4/$KMnO_4$ treatment (Figure 6D), whereas the FA generated by [4,5-^{3}H]DHS labeling migrated to a position identical to that of palmitic acid (Figure 6C). These results indicate that the Δ*faa1* Δ*faa4* cells accumulated hexadecenoic acid as a [11,12-^{3}H]Sph metabolite, which is in contrast to wild type cells, in which [11,12-^{3}H]Sph was metabolized to palmitic acid, a constituent of glycerolipids (Figure 4D and E). Considering that hexadecenoic acid is a substrate of the ACSs Faa1 and Faa4, the product should be hexadecenoyl-CoA. Thus, it is most probable that hexadecenoyl-CoA is converted to palmitoyl-CoA before incorporation into glycerolipids.

We next investigated the sensitivity of the Δ*faa1* Δ*faa4* cells to exogenous LCBs, and

compared it to that of the other tested mutants. In contrast to the Δ*hfd1* cells, the Δ*faa1* Δ*faa4* cells were not sensitive to exogenous DHS or Sph, indicating that accumulated hexadecenoic acid is not toxic to these cells (Figure S3B). Thus, toxic fatty aldehydes are detoxified by Hfd1.

Of the 26 mammalian ACSs, Faa1 and Faa4 share the highest homology with the ACSL subfamily members ACSL1, 3, 4, 5, and 6, with ACSL4 exhibiting the highest similarity overall (26.6% identity and 47.7% similarity to Faa1 and 30.3% identity and 47.9% similarity to Faa4). When these proteins were expressed in Δ*faa1* Δ*faa4* cells as N-terminally 3xFLAG tagged proteins, all restored Sph-to-glycerolipid conversion (Figure 6E). However, two other ACS subfamily members, ACSS1 and ACSM1, exhibited no activity, and restoration was weak for ACSL3, probably due to low expression levels (Figure 6F). These results indicate that ACSL family members can also convert hexadecenoic acid to hexadecenoyl-CoA, in a manner similar to that observed for yeast Faa1 and Faa4.

DISCUSSION

Aside from its well-known function as a bioactive lipid molecule, S1P is also important as an intermediate in the sphingolipid-to-glycerolipid conversion pathway. However, certain steps in this metabolic pathway, and the metabolic enzymes involved with those steps, remain unresolved. At least three pathways were considered in studying the conversion of hexadecenal (the product of S1P by S1P lyase) to palmitoyl-CoA (Figure S5, Schemes 1 to 3). It is possible that hexadecenal is first converted to hexadecanal, then to palmitic acid, and finally to palmitoyl-CoA (Figure S5, Scheme 1). Alternatively, hexadecenal is converted to palmitoyl-CoA via hexadecenoic acid and hexadecenoyl-CoA (Scheme 2) or via hexadecenoic acid and palmitic acid (Scheme 3). Our results clearly indicate that Scheme 2 (also shown in Figure 7) is the actual S1P metabolic pathway. Aldehyde molecules are highly reactive, so they must be immediately metabolized to other non-toxic compounds, in this case carboxylic acid. Indeed, we demonstrated such toxic effects by fatty aldehydes and non-toxic effects of carboxylic acids by examining the LCB sensitivity of Δ*hfd1* and Δ*faa1* Δ*faa4* cells (Figure S3). If hexadecenal was not rapidly metabolized, but instead was first converted to hexadecanal, as shown in Scheme 1 in Figure S5, toxic effects from these aldehydes might occur.

The hexadecenoic acid generated is converted to hexadecenoyl-CoA (Figure S5, Scheme 2), but not to palmitic acid (Figure S5, Scheme 3), as indicated by the yeast mutant of acyl-CoA synthetases (Δ*faa1* Δ*faa4*), which accumulated hexadecenoic acid but not palmitic acid (Figure 6C and D). If the metabolism followed Scheme 3, the intermediate in the acyl-CoA synthetase-null yeast cells would be palmitic acid.

The ER is the major organelle responsible for synthesizing and metabolizing lipids. LCBPs are degraded by S1P/LCBP lyase or S1P/LCBP phosphatase in the ER (Ikeda et al., 2004; Kihara and Igarashi, 2008). Likewise, ALDH3A2 is also localized in the ER (Ashibe et al., 2007). In addition, localization of Faa1, Faa4, and ACSLs in the ER has been reported

(Natter et al., 2005; Soupene and Kuypers, 2008). Thus, the entire S1P metabolism pathway found in this study occurs in the ER. The ER also contains a *trans*-2,3-enoyl-CoA reductase (Tsc13 in yeast and TER in mammals), which functions in FA elongation (Kohlwein et al., 2001; Moon and Horton, 2003). Since hexadecenoyl-CoA derived from S1P is also a *trans*-2,3-enoyl-CoA, these *trans*-enoyl-CoA reductases might be responsible for the conversion of hexadecenoyl-CoA to palmitoyl-CoA.

LCBs were metabolized to both sphingolipids and glycerolipids in wild type yeast cells, while the glycerolipid pathway was completely blocked in Δ*hfd1* cells (Figure 2A). In contrast, LCBs were still converted to glycerolipids, although in reduced amounts, in mammalian cells lacking ALDH3A2 (FAA-K1A cells; Figure 5B). Furthermore, in FAA-K1A cells LCBs were apparently metabolized to the *sn*-2 acyl group of plasmanylcholine/plasmenylethanolamine, in addition to the *sn*-1 alkyl/alkenyl groups (Figure 5B). Reportedly, FAA-K1A cells exhibit ~10% FALDH activity compared to wild type CHO-K1 cells (James and Zoeller, 1997). It is possible that trace amounts of the *ALDH3A2* mRNA, below the detection limit of our RT-PCR (Figure 5A) are expressed in FAA-K1A cells. Alternatively, another FALDH, perhaps another ALDH3 family member, might be responsible for the residual FALDH activity. In FAA-K1A cells, some LCBs were metabolized to the ether-linked glycerolipids plasmenylethanolamine and plasmanylcholine (Figure 5B). Generation of these lipids require fatty alcohols as substrates (Nagan and Zoeller, 2001). Cellular fatty alcohols are mainly produced from acyl-CoAs by the fatty acyl-CoA reductase Far1 (Honsho et al., 2010), and are utilized in the production of ether-linked glycerolipids or are converted to FAs via fatty aldehydes by a fatty alcohol:NAD oxidoreductase (FAO) complex (Lee, 1979). Although fatty alcohol dehydrogenase in the FAO complex normally catalyzes the conversion of fatty alcohol to fatty aldehyde, accumulation of fatty aldehydes in FAA-K1A cells may cause an equilibration shift, resulting in a reverse reaction. Although the metabolic pathway for LCB to ether-linked

glycerolipids was observed only in the *ALDH3A2*-null FAA-K1A cells, it is possible that this pathway also functions in certain tissues or cell types where expression levels of ALDH3A2 are low.

In the pathology of SLS, accumulated fatty aldehyde molecules normally metabolized by ALDH3A2 are thought to react with important cellular components and cause cell damage (Rizzo, 2007). However, the identity of the pathology-causing fatty aldehydes and their origins still remain unclear, although several candidate molecules/pathways have been proposed, including phytol oxidation (van den Brink et al., 2004) and the leukotriene B_4 metabolic pathway (Willemsen et al., 2001). We propose here that hexadecenal derived from S1P may contribute to the pathology of SLS, at least partly. Considerable amounts of glycerolipids were detected by [11,12-^{3}H]Sph or [4,5-^{3}H]DHS labeling in all cells tested here (HEK 293T, F9, and CHO-K1 cells) (Figure 3C and D and Figure 5B). Moreover, Sph kinase, S1P lyase, and ALDH3A2 are all ubiquitously expressed (Ikeda et al., 2004; Liu et al., 2000; Nava et al., 2000; Rogers et al., 1997), so the Sph/S1P-to-glycerolipid metabolic pathway may be active in most tissues. Thus, we speculate that hexadecenal derived from S1P may account for a relatively large proportion of intracellularly generated fatty aldehydes.

In the presented study, we revealed the entire S1P metabolic pathway. However, future study is required for the identification of the still missing reductase responsible for converting hexadecenoyl-CoA to palmitoyl-CoA. In addition, the S1P metabolite hexadecenal and its involvement in the pathogenesis of SLS should be investigated using *Aldh3A2* knockout mice.

EXPERIMENTAL PROCEDURES

Yeast Strains, Plasmids, Cell Culture, and Transfection

Cell lines, culture media, and transfection reagents used, as well as construction of *S. cerevisiae* strains and of plasmids, are described in the Supplemental Information.

Immunological Assays

Immunoblotting was performed as described previously (Kihara et al., 2006).

[11,12-^{3}H]Sph Preparation

[11,12-^{3}H]Sph was generated from [9,10-^{3}H]palmitic acid using HEK 293T cells. HEK 293T cells were labeled for 24 hr at 37 ˚C with 3 mCi [9,10-^{3}H]palmitic acid (40 Ci/mmol, 10 mCi/ml; American Radiolabeled Chemicals (ARC), St. Louis, MO). Cells were washed with PBS, suspended in 6 ml PBS with 5 mM dithiothreitol, and transferred to glass tubes. Lipids were extracted by successive addition and mixing of 22.5 ml chloroform/methanol/HCl (100:200:1, v/v), 7.5 ml chloroform, and 7.5 ml 1% KCl. Phases were separated by centrifugation, and the organic phase was recovered, dried, and suspended in 3.6 ml chloroform/methanol (1:1, v/v) with 1% buthylhydroxytoluene. Samples were then incubated with methanolysis reagent (4 ml 10% methanolic HCl and 0.4 ml 2,2-dimethoxypropane) for 5 hr at 100 ˚C. Generated FA methyl esters were removed from methanol with 8 ml hexane. Phases were separated by centrifugation, and the hexane phase was discarded. After repeating the hexane extraction thrice, lipids were extracted from the methanol phase by successive addition and mixing of 6 ml chloroform and 6 ml 1% KCl. After phase separation by centrifugation, the organic phase was recovered, dried, and suspended in 200 μl chloroform /methanol (1:1, v/v). Lipids were resolved by TLC on Silica Gel 60 HPTLC plates (Merck, Whitestation, NJ) with chloroform/methanol/4.2 N ammonia (9:7:2, v/v) so the leading edge

was positioned 1.5 cm below the top. Plates were then dried and resolved with chloroform/methanol/15 N ammonia (60:12:1, v/v) to the top. Sph was scraped from the TLC plate and was extracted once using 300 μl ethanol with 0.2 N ammonia and three times using 100 μl ethanol with 0.2 N ammonia. Silica gel was removed by centrifugation, and the collected lipids were combined, dried, and suspended in 30 μl ethanol. Typically, 400-600 μM Sph carrying a 0.15-0.4 μCi/μl label was obtained by this method.

[^{3}H]LCB Labeling Assays

Yeast cells were labeled with [11,12-^{3}H]Sph or [4,5-^{3}H]DHS (ARC) essentially as described previously (Kihara et al., 2008). Double bond cleavage assays were performed essentially as described elsewhere (Scarim et al., 1989). Cultured mammalian cells were labeled with [11,12-^{3}H]Sph or [4,5-^{3}H]DHS as described previously (Kihara et al., 2003). Details are described in the Supplemental Information.

***In Vitro* Enzyme Assays**

3xFLAG-SPHK1, 3xFLAG-SPL, or 3xFLAG-ALDH3A2 was expressed in HEK 293T cells, then affinity-purified using anti-FLAG M2 affinity agarose gel. HEK 293T cells were transfected with the pCE-puro 3xFLAG-mSPHK1a, pCE-puro 3xFLAG-mSPL, or pCE-puro 3xFLAG-ALDH3A2 plasmid. Twenty-four hr after transfection, cells were suspended in buffer A (50 mM HEPES-NaOH (pH 7.4), 150 mM NaCl, 10% glycerol, 1x protease inhibitor mixture (Complete^{TM} EDTA free; Roche Diagnostics, Indianapolis, IN), 1 mM phenylmethylsulfonyl fluoride, and 1 mM dithiothreitol) and lysed by sonication. The resulting total cell lysates were subjected to centrifugation at 100,000 g for 30 min at 4 ˚C. The supernatant (soluble fraction) was used for purification of 3xFLAG-SPHK1, and the pellet (membrane fraction) was used for purification of 3xFLAG-SPL and 3xFLAG-ALDH3A2. The

pellet was suspended in buffer A by sonication and solubilized with 1% Triton X-100 for 30 min at 4 ˚C. After centrifugation at 100,000 g for 30 min at 4 ˚C, the supernatant (solubilized fraction) was recovered. Anti-FLAG M2 affinity agarose gel was added to the soluble fraction containing 3xFLAG-SPHK1 or to the solubilized fraction containing 3xFLAG-SPL or 3xFLAG-ALDH3A2, and each mixture was incubated over night at 4 ˚C with rotation. Beads were washed twice with buffer A (for 3xFLAG-SPHK1) or buffer A containing 0.1% Triton X-100 (for 3xFLAG-SPL and 3xFLAG-ALDH3A2); bound proteins were eluted with buffer A containing 100 μg/ml 3xFLAG peptide with 0.1% Triton X-100 (for 3xFLAG-SPL and 3xFLAG-ALDH3A2) or without (for 3xFLAG-SPHK1).

Sph kinase assays and [11,12-^{3}H]S1P preparation were performed as described previously (Kihara et al., 2003). *In vitro* FALDH assays were performed using hexadecanal (Kariya et al., 2005) and 2-*trans*-hexadecenal (Avanti Polar Lipid, Alabaster, AL) as described elsewhere (Kelson et al., 1997).

For use as a TLC standard, [9,10-^{3}H]hexadecenoic acid was prepared from [11,12-^{3}H]S1P using affinity purified 3xFLAG-SPL and 3xFLAG-ALDH3A2. 3xFLAG-SPL and 3xFLAG-ALDH3A2 were incubated for 1 hr at 37 ˚C with [11,12-^{3}H]S1P, complexed with 1 mg/ml (final concentration of 0.2 mg/ml) FA-free BSA, in buffer A containing 0.1% Triton X-100, 100 μM NAD^{+}, and 250 μM pyridoxal 5'-phosphate. After the reaction, lipids were extracted, dried, and suspended in ethanol.

RT-PCR

RT-PCR was performed using a Super Script One-Step RT-PCR with Platinum Taq (Invitrogen) and primers described in the Supplemental Information.

SUPPLEMENTAL INFORMATION

Supplemental Information includes five figures, Supplemental Experimental Procedures, and Supplemental References.

ACKNOWLEDGMENTS

This work was supported by a Grant-in-Aid for Scientific Research on Innovative Areas (23116501) from the Ministry of Education, Culture, Sports, Sciences and Technology of Japan. We are grateful to Dr. E. A. Sweeney and Dr. T. Toyokuni for scientific editing of the manuscript.

REFERENCES

Ashibe, B., Hirai, T., Higashi, K., Sekimizu, K., and Motojima, K. (2007). Dual subcellular localization in the endoplasmic reticulum and peroxisomes and a vital role in protecting against oxidative stress of fatty aldehyde dehydrogenase are achieved by alternative splicing. J. Biol. Chem. *282*, 20763-20773.

Black, P.N., and DiRusso, C.C. (2007). Yeast acyl-CoA synthetases at the crossroads of fatty acid metabolism and regulation. Biochim. Biophys. Acta *1771*, 286-298.

De Laurenzi, V., Rogers, G.R., Hamrock, D.J., Marekov, L.N., Steinert, P.M., Compton, J.G., Markova, N., and Rizzo, W.B. (1996). Sjögren-Larsson syndrome is caused by mutations in the fatty aldehyde dehydrogenase gene. Nat. Genet. *12*, 52-57.

Honsho, M., Asaoku, S., and Fujiki, Y. (2010). Posttranslational regulation of fatty acyl-CoA reductase 1, Far1, controls ether glycerophospholipid synthesis. J. Biol. Chem. *285*, 8537-8542.

Ikeda, M., Kihara, A., and Igarashi, Y. (2004). Sphingosine-1-phosphate lyase SPL is an endoplasmic reticulum-resident, integral membrane protein with the pyridoxal 5'-phosphate binding domain exposed to the cytosol. Biochem. Biophys. Res. Commun. *325*, 338-343.

Ikeda, M., Kihara, A., Kariya, Y., Lee, Y.M., and Igarashi, Y. (2005). Sphingolipid-to-glycerophospholipid conversion in *SPL*-null cells implies the existence of an alternative isozyme. Biochem. Biophys. Res. Commun. *329*, 474-479.

James, P.F., and Zoeller, R.A. (1997). Isolation of animal cell mutants defective in long-chain fatty aldehyde dehydrogenase. Sensitivity to fatty aldehydes and Schiff's base modification of phospholipids: implications for Sjögren-Larsson syndrome. J. Biol. Chem. *272*, 23532-23539.

Kariya, Y., Kihara, A., Ikeda, M., Kikuchi, F., Nakamura, S., Hashimoto, S., Choi, C.H., Lee,

Y.M., and Igarashi, Y. (2005). Products by the sphingosine kinase/sphingosine 1-phosphate (S1P) lyase pathway but not S1P stimulate mitogenesis. Genes Cells *10*, 605-615.

Kelson, T.L., Secor McVoy, J.R., and Rizzo, W.B. (1997). Human liver fatty aldehyde dehydrogenase: microsomal localization, purification, and biochemical characterization. Biochim. Biophys. Acta *1335*, 99-110.

Kihara, A., Anada, Y., and Igarashi, Y. (2006). Mouse sphingosine kinase isoforms SPHK1a and SPHK1b differ in enzymatic traits including stability, localization, modification, and oligomerization. J. Biol. Chem. *281*, 4532-4539.

Kihara, A., and Igarashi, Y. (2008). Production and release of sphingosine 1-phosphate and the phosphorylated form of the immunomodulator FTY720. Biochim. Biophys. Acta *1781*, 496-502.

Kihara, A., Ikeda, M., Kariya, Y., Lee, E.Y., Lee, Y.M., and Igarashi, Y. (2003). Sphingosine-1-phosphate lyase is involved in the differentiation of F9 embryonal carcinoma cells to primitive endoderm. J. Biol. Chem. *278*, 14578-14585.

Kihara, A., Mitsutake, S., Mizutani, Y., and Igarashi, Y. (2007). Metabolism and biological functions of two phosphorylated sphingolipids, sphingosine 1-phosphate and ceramide 1-phosphate. Prog. Lipid Res. *46*, 126-144.

Kihara, A., Sakuraba, H., Ikeda, M., Denpoh, A., and Igarashi, Y. (2008). Membrane topology and essential amino acid residues of Phs1, a 3-hydroxyacyl-CoA dehydratase involved in very long-chain fatty acid elongation. J. Biol. Chem. *283*, 11199-11209.

Kohlwein, S.D., Eder, S., Oh, C.S., Martin, C.E., Gable, K., Bacikova, D., and Dunn, T. (2001). Tsc13p is required for fatty acid elongation and localizes to a novel structure at the nuclear-vacuolar interface in *Saccharomyces cerevisiae*. Mol. Cell. Biol. *21*, 109-125.

Kolesnick, R.N., and Krönke, M. (1998). Regulation of ceramide production and apoptosis.

Annu. Rev. Physiol. *60*, 643-665.

Lee, T. (1979). Characterization of fatty alcohol:NAD^+ oxidoreductase from rat liver. J. Biol. Chem. *254*, 2892-2896.

Liu, H., Sugiura, M., Nava, V.E., Edsall, L.C., Kono, K., Poulton, S., Milstien, S., Kohama, T., and Spiegel, S. (2000). Molecular cloning and functional characterization of a novel mammalian sphingosine kinase type 2 isoform. J. Biol. Chem. *275*, 19513-19520.

Moon, Y.A., and Horton, J.D. (2003). Identification of two mammalian reductases involved in the two-carbon fatty acyl elongation cascade. J. Biol. Chem. *278*, 7335-7343.

Nagan, N., and Zoeller, R.A. (2001). Plasmalogens: biosynthesis and functions. Prog. Lipid Res. *40*, 199-229.

Natter, K., Leitner, P., Faschinger, A., Wolinski, H., McCraith, S., Fields, S., and Kohlwein, S.D. (2005). The spatial organization of lipid synthesis in the yeast *Saccharomyces cerevisiae* derived from large scale green fluorescent protein tagging and high resolution microscopy. Mol. Cell. Proteomics *4*, 662-672.

Nava, V.E., Lacana, E., Poulton, S., Liu, H., Sugiura, M., Kono, K., Milstien, S., Kohama, T., and Spiegel, S. (2000). Functional characterization of human sphingosine kinase-1. FEBS Lett. *473*, 81-84.

Pyne, S., and Pyne, N.J. (2011). Translational aspects of sphingosine 1-phosphate biology. Trends Mol. Med. *17*, 463-472.

Rizzo, W.B. (2007). Sjögren-Larsson syndrome: molecular genetics and biochemical pathogenesis of fatty aldehyde dehydrogenase deficiency. Mol. Genet. Metab. *90*, 1-9.

Rogers, G.R., Markova, N.G., De Laurenzi, V., Rizzo, W.B., and Compton, J.G. (1997). Genomic organization and expression of the human fatty aldehyde dehydrogenase gene (FALDH). Genomics *39*, 127-135.

Scarim, J., Ghanbari, H., Taylor, V., and Menon, G. (1989). Determination of

phosphatidylcholine and disaturated phosphatidylcholine content in lung surfactant by high performance liquid chromatography. J. Lipid Res. *30*, 607-611.

Sillence, D.J., and Platt, F.M. (2003). Storage diseases: new insights into sphingolipid functions. Trends Cell Biol. *13*, 195-203.

Soupene, E., and Kuypers, F.A. (2008). Mammalian long-chain acyl-CoA synthetases. Exp. Biol. Med. *233*, 507-521.

Stoffel, W., and Sticht, G. (1967). Metabolism of sphingosine bases, I. Degradation and incorporation of [3-^{14}C]*erythro*-DL-dihydrosphingosine and [7-$^{3}H_2$]*erythro*-DL-sphingosine into sphingolipids of rat liver. Hoppe Seylers Z. Physiol. Chem. *348*, 941-943.

Tani, M., Kihara, A., and Igarashi, Y. (2006). Rescue of cell growth by sphingosine with disruption of lipid microdomain formation in *Saccharomyces cerevisiae* deficient in sphingolipid biosynthesis. Biochem. J. *394*, 237-242.

van den Brink, D.M., van Miert, J.N., Dacremont, G., Rontani, J.F., Jansen, G.A., and Wanders, R.J. (2004). Identification of fatty aldehyde dehydrogenase in the breakdown of phytol to phytanic acid. Mol. Genet. Metab. *82*, 33-37.

Watkins, P.A., Maiguel, D., Jia, Z., and Pevsner, J. (2007). Evidence for 26 distinct acyl-coenzyme A synthetase genes in the human genome. J. Lipid Res. *48*, 2736-2750.

Willemsen, M.A., Rotteveel, J.J., de Jong, J.G., Wanders, R.J., L, I.J., Hoffmann, G.F., and Mayatepek, E. (2001). Defective metabolism of leukotriene B_4 in the Sjogren-Larsson syndrome. J. Neurol. Sci. *183*, 61-67.

Zhang, X., Skrzypek, M.S., Lester, R.L., and Dickson, R.C. (2001). Elevation of endogenous sphingolipid long-chain base phosphates kills *Saccharomyces cerevisiae* cells. Curr. Genet. *40*, 221-233.

FIGURE LEGENDS

Figure 1 The Sphingolipid Synthesis Pathway of Mammals and Yeast.

(A) The sphingolipid biosynthetic and metabolic pathways of mammals are shown. S1P and DHS1P are metabolized to palmitoyl-CoA and further to glycerolipids. DHS1P is metabolized to palmitoyl-CoA via hexadecanal and palmitic acid, but the entire S1P to palmitoyl-CoA metabolic pathway is not fully known. (B) The sphingolipid biosynthetic and metabolic pathways of yeast are shown. As in mammals, the biosynthesis of sphingolipids begins with the condensation of serine with acyl-CoA to form 3-ketodihydrosphingosine, which is then reduced to DHS and acylated to dihydroceramide. In mammalian cells, a 4,5-*trans*-double bond is then incorporated to form Cer, which is further converted to sphingomyelin or glycosphingolipids. However, in yeast the double bond is not introduced; instead a hydroxy group is attached to the 4-position of DHS, generating phytosphingosine. Phytosphingosine and some DHS are then converted to Cers (dihydroceramide and phytoceramide) and further to inositol-containing complex sphingolipids, specifically IPC, MIPC, and $M(IP)_2C$. The DHS1P-to-glycerolipid metabolic pathway is conserved between yeast and mammals.

Figure 2 Yeast Hfd1 and Human ALDH3A2 Are FALDHs Involved in the LCB/LCBP Metabolism.

(A and B) Wild type or mutant yeast cells were labeled with [4,5-^{3}H]DHS, and lipids were extracted and separated by TLC with chloroform/methanol/4.2 N ammonia (9:7:2, v/v) then chloroform/methanol/15 N ammonia (60:12:1, v/v). (A) BY4741 wild type cells, and 3653 (Δ*dpl1*), 6550 (Δ*hfd1*), 753 (Δ*ald2*), 6071 (Δ*ald3*), 1671 (Δ*ald4*), 213 (Δ*ald5*), 2767 (Δ*ald6*), 3141 (Δ*uga2*), and 1002 (Δ*msc7*) mutant cells grown in YPD medium were labeled with 0.1 μCi [4,5-^{3}H]DHS for 2 hr at 30 ˚C. (B) BY4741 cells bearing pAKNF316 (vector; BY4741/pAKNF316), 6550 (Δ*hfd1*)/pAKNF316 cells, and 6550/pNK5 (*3xFLAG-ALDH3A2*)

cells grown in SC medium lacking uracil were labeled with 0.1 μCi [4,5-^{3}H]DHS for 3 hr at 30 ˚C. Multiple independent experiments (4 for (A) and 3 for (B)) gave similar results for each assay, and a representative result is shown for each. HaOH, hexadecanol. See also Figure S1.

Figure 3 Preparation of Traceable [11,12-^{3}H]Sph and Its Metabolism in Mammalian Cells. (A) [11, 12-^{3}H]Sph prepared in this study and [3-^{3}H]Sph and [4,5-^{3}H]DHS purchased from ARC, each at 0.016 μCi, were separated by TLC. (B) [11, 12-^{3}H]Sph (0.016 μCi) was incubated with or without the Sph kinase 3xFLAG-SPHK1a for 1 hr at 37 ˚C. Lipids were extracted then separated by TLC with chloroform/methanol/4.2 N ammonia (9:7:2, v/v) then chloroform/methanol/15 N ammonia (60:12:1, v/v). (C) HEK 293T cells were labeled with 0.25 μCi [11,12-^{3}H]Sph or [4,5-^{3}H]DHS for 4 hr at 37 ˚C. Lipids were extracted, treated with nothing or alkaline solution, and separated by TLC with 1-butanol/acetic acid/ water (3:1:1, v/v). (D) Mouse embryonic carcinoma F9 (wild type) and F9-2 (*SPL*$^{-/-}$) cells were labeled with 0.08 μCi [11,12-^{3}H]Sph or [4,5-^{3}H]DHS for 2 hr or 24 hr at 37 ˚C. Lipids were extracted then separated by TLC with 1-butanol/acetic acid/ water (3:1:1, v/v). Multiple independent experiments (4 each for (A) and (B), 3 for (C), and 2 for (D)) gave similar results for each assay, and a representative result is shown for each. SM, sphingomyelin. See also Figure S2.

Figure 4 Sph to Glycerolipid Metabolic Pathways Are Conserved between Yeast and Mammals.

(A and B) Wild type and mutant yeast cells were labeled with radioactive LCBs, then lipids were extracted, treated with nothing or alkaline solution, and separated by TLC with chloroform/methanol/4.2 N ammonia (9:7:2, v/v). (A) Yeast wild type BY4741 cells and 3653 (Δ*dpl1*) and 6550 (Δ*hfd1*) mutant cells were labeled with 0.08 μCi [4,5-^{3}H]DHS or [11,12-^{3}H]Sph for 3 hr at 30 ˚C. (B) BY4741 (wild type)/pAKNF316 (vector), 6550

(Δ*hfd1*)/pAKNF316, and 6550/pNK5 (*3xFLAG-ALDH3A2*) cells grown in SC medium lacking uracil were labeled with 0.08 μCi [11,12-^{3}H]Sph for 3 hr at 30 ˚C. (C) Affinity-purified 3xFLAG-ALDH3A2 (50 ng) was incubated with 500 μM NAD^+ and 100 μM hexadecanal or hexadecenal for 20 min at 37 ˚C. The fluorescence of the produced NADH (excitation at 356 nm and emission at 460 nm) was measured using a Spectrofluorophotometer RF-1500 (Shimazu, Kyoto, Japan). FALDH activities shown represent the mean ± SD from three independent experiments. (D and E) HEK 293T mammalian cells were labeled with 0.08 μCi [4,5-^{3}H]DHS or [11,12-^{3}H]Sph for 4 hr at 37 ˚C, and yeast BY4741 cells were labeled with 0.08 μCi [4,5-^{3}H]DHS or [11,12-^{3}H]Sph for 3 hr at 30 ˚C. Lipids were extracted and subjected to alkaline treatment. (D) [2,3-^{3}H]Palmitic acid and [9,10-^{3}H]2-*trans*-hexadecenoic acid were prepared by incubating [4,5-^{3}H]DHS1P and [11,12-^{3}H]S1P with 3xFLAG-SPL and 3xFLAG-ALDH3A2, respectively, for 30 min at 37 ˚C. [9,10-^{3}H]Palmitic acid was purchased from ARC. Lipids were separated by TLC with hexane/diethyl ether/acetic acid (30:70:1, v/v). Note that, other than FAs, no labeled lipids were moved from the origin by this highly nonpolar resolving buffer. (E) Lipids were left untreated or were treated with $KMnO_4/KIO_4$, then were methyl-esterified, extracted with hexane, and separated by reverse-phase TLC with chloroform/methanol/water (5:15:1, v/v). Multiple independent experiments (3 for (A) and 2 each for (B), (D), and (E)) gave similar results for each assay, and a representative result is shown for each. HaOH, hexadecanol; HeOH, hexadecenol; PA, palmitic acid; HA, hexadecenoic acid; HEK, HEK 293T cells. See also Figure S3.

Figure 5 LCBs Are Metabolized to Ether-linked Glycerolipids in *ALDH3A2*-deficient CHO-K1 Cells.

(A) Total RNAs prepared from CHO-K1 and FAA-K1A cells were subjected to RT-PCR using primers specific for *ALDH3A2*. Amplified DNA fragments were separated by agarose gel

electrophoresis and stained with ethidium bromide. *Glyceraldehyde 3-phosphate dehydrogenase* (*GAPDH*) was used as a loading control. (B) CHO-K1 and FAA-K1A cells were labeled with 0.125 μCi [4,5-^{3}H]DHS or [11,12-^{3}H]Sph for 4 hr at 37 ˚C. Lipids were extracted, treated with nothing, 0.2 M NaOH, or 40 mM HCl for 1 hr at 37˚C. The mixtures were neutralized, then lipids were re-extracted and separated by TLC with 1-butanol/acetic acid/ water (3:1:1, v/v). Three independent experiments gave similar results for each reaction, and a representative result is shown for each. Plasmenyl-E, plasmenylethanolamine; Plasmanyl-C, plasmanylcholine; SM, sphingomyelin. See also Figure S4.

Figure 6 Hexadecenoic Acid Is an Intermediate in the Sph-to-glycerolipid Metabolic Pathway in Acyl-CoA Synthetase-deficient Yeast Cells.

(A) Wild type BY4741 cells, and 6477 (Δ*faa1*), AOY9 (Δ*faa2*), AOY10 (Δ*faa3*), 833 (Δ*faa4*), 3178 (Δ*fat1*), 3362 (Δ*fat2*), 6868 (Δ*acs1*), AOY11 (Δ*faa1* Δ*faa2*), AOY12 (Δ*faa1* Δ*faa3*), and AOY13 (Δ*faa1* Δ*faa4*) mutant cells grown in YPD medium were labeled with 0.1 μCi [4,5-^{3}H]DHS for 2 hr at 30 ˚C. Lipids were extracted and separated by TLC with chloroform/methanol/4.2 N ammonia (9:7:2, v/v) then chloroform/methanol/15 N ammonia (60:12:1, v/v). (B, C, and D) Wild type BY4741 cells and AOY13 (Δ*faa1* Δ*faa4*) cells were labeled with [4,5-^{3}H]DHS or [11,12-^{3}H]Sph for 2 hr at 30 ˚C. Lipids were extracted and separated by TLC with chloroform/methanol/4.2 N ammonia (9:7:2, v/v) then chloroform/methanol/15 N ammonia (60:12:1, v/v) (B) or hexane/diethyl ether/acetic acid (30:70:1, v/v) (C). [2,3-^{3}H]Palmitic acid, [9,10-^{3}H]2-*trans*-hexadecenoic acid, and [9,10-^{3}H]palmitic acid were also separated by TLC in (C). [2,3-^{3}H]Palmitic acid and [9,10-^{3}H]2-*trans*-hexadecenoic acid were prepared by incubating [4,5-^{3}H]DHS1P and [11,12-^{3}H]S1P with 3xFLAG-SPL and 3xFLAG-ALDH3A2, respectively, for 30 min at 37 ˚C. [9,10-^{3}H]Palmitic acid was purchased from ARC. Note that, other than FAs, no labeled lipids

were moved from the origin by this highly nonpolar resolving buffer. PA, palmitic acid; HA, hexadecenoic acid. (D) Lipids prepared from AOY13 (Δ*faa1* Δ*faa4*) cells labeled with [11,12-^{3}H]Sph were left untreated or were treated with $KMnO_4/KIO_4$, then were methyl-esterified, extracted with hexane, and separated by reverse-phase TLC with chloroform/methanol/water (5:15:1, v/v). (E and F) AOY13 (Δ*faa1* Δ*faa4*) mutant cells were transfected with a pAKNF316 (vector), pAO15 (*3xFLAG-ACSL1*), pAO16 (*3xFLAG-ACSL3*), pAO17 (*3xFLAG-ACSL4*), pAO19 (*3xFLAG-ACSL5*), pAO21 (*3xFLAG-ACSL6*), pAO25 (*3xFLAG-ACSS1*), or pAO26 (*3xFLAG-ACSM1*) plasmid. (E) Cells were labeled with [11,12-^{3}H]Sph for 2 hr at 30 ˚C. Lipids were extracted and separated by TLC with chloroform/methanol/4.2 N ammonia (9:7:2, v/v). (F) Cell lysates were prepared and subjected to immunoblot analysis with an anti-FLAG antibody or, to demonstrate uniform protein loading, an anti-Pgk1 antibody. Two independent experiments gave similar results for each assay, and a representative result is shown for each.

Figure 7 The S1P Metabolic Pathway Revealed in This Study.

The pathway and enzymes responsible for S1P metabolism revealed in the present study are shown. The underlined enzymes indicate yeast proteins. See also Figure S5.

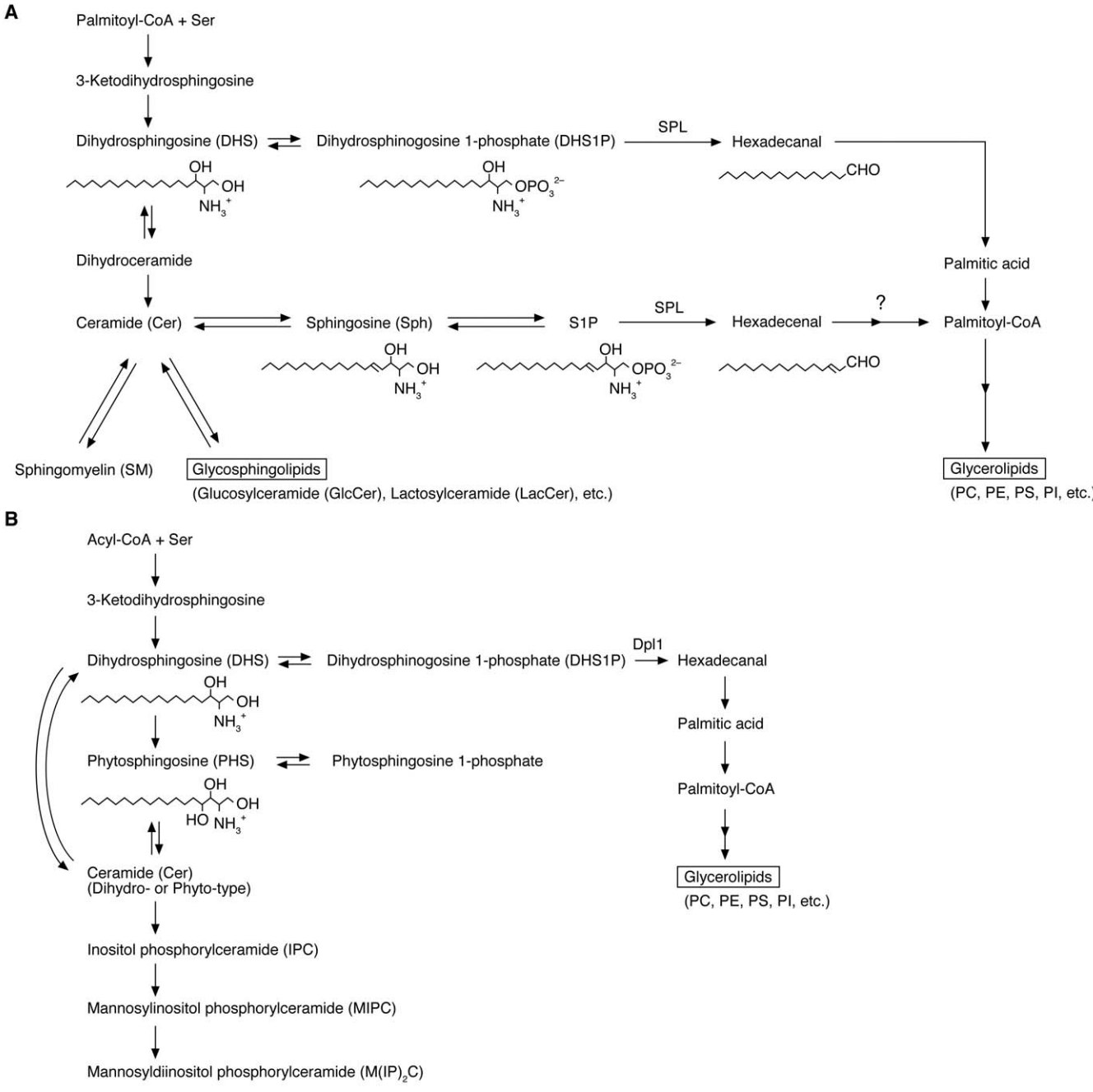
A
Palmitoyl-CoA + Ser
3-Ketodihydrosphingosine
Dihydrosphingosine (DHS)
Dihydrosphinogosine 1-phosphate (DHS1P)
SPL
Hexadecanal
Dihydroceramide
Palmitic acid
Ceramide (Cer)
Sphingosine (Sph)
S1P
SPL
Hexadecenal
?
Palmitoyl-CoA
Sphingomyelin (SM)
Glycosphingolipids
(Glucosylceramide (GlcCer), Lactosylceramide (LacCer), etc.)
Glycerolipids
(PC, PE, PS, PI, etc.)
B
Acyl-CoA + Ser
3-Ketodihydrosphingosine
Dihydrosphingosine (DHS)
Dihydrosphinogosine 1-phosphate (DHS1P)
Dpl1
Hexadecanal
Palmitic acid
Palmitoyl-CoA
Phytosphingosine (PHS)
Phytosphingosine 1-phosphate
Ceramide (Cer)
(Dihydro- or Phyto-type)
Glycerolipids
(PC, PE, PS, PI, etc.)
Inositol phosphorylceramide (IPC)
Mannosylinositol phosphorylceramide (MIPC)
Mannosyldiinositol phosphorylceramide (M(IP)2C)

Fig. 1

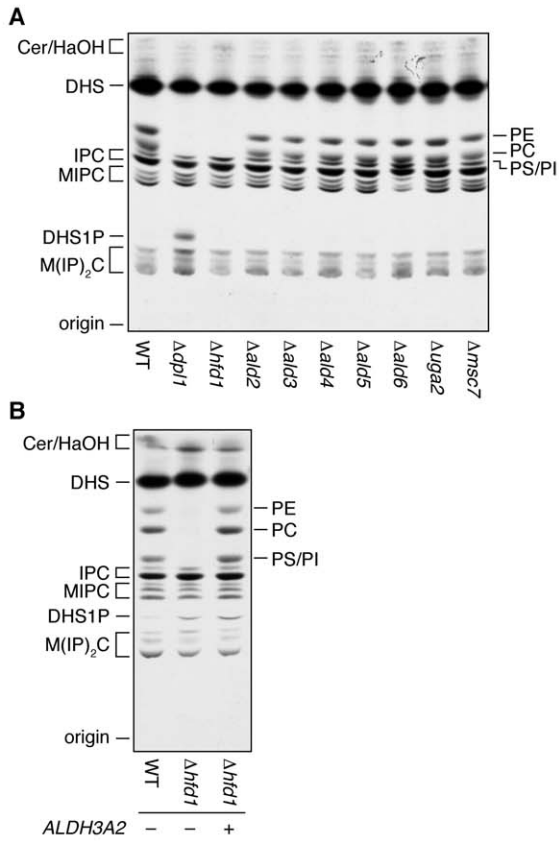
A
Cer/HaOH
DHS
IPC
MIPC
DHS1P
M(IP)2C
origin
PE
PC
PS/PI
WT
Δdpl1
Δhfd1
Δald2
Δald3
Δald4
Δald5
Δald6
Δuga2
Δmsc7
B
Cer/HaOH
DHS
IPC
MIPC
DHS1P
M(IP)2C
origin
PE
PC
PS/PI
WT
Δhfd1
Δhfd1
ALDH3A2
–
–
+

Fig. 2

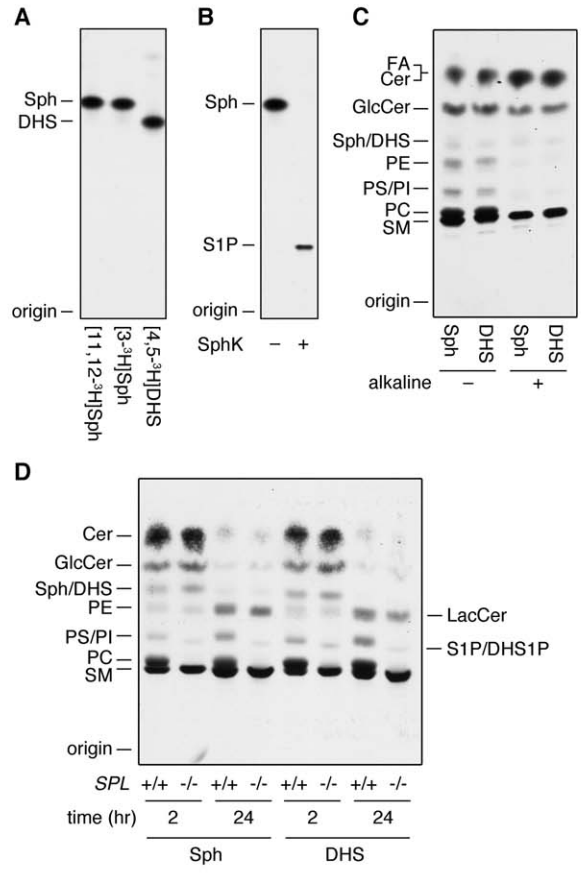
A
Sph
DHS
origin
[11,12-³H]Sph
[3-³H]Sph
[4,5-³H]DHS
B
Sph
S1P
origin
SphK – +
C
FA
Cer
GlcCer
Sph/DHS
PE
PS/PI
PC
SM
origin
Sph
DHS
Sph
DHS
alkaline – +
D
Cer
GlcCer
Sph/DHS
PE
PS/PI
PC
SM
origin
LacCer
S1P/DHS1P
SPL +/+ -/- +/+ -/- +/+ -/- +/+ -/-
time (hr) 2 24 2 24
Sph
DHS

Fig. 3

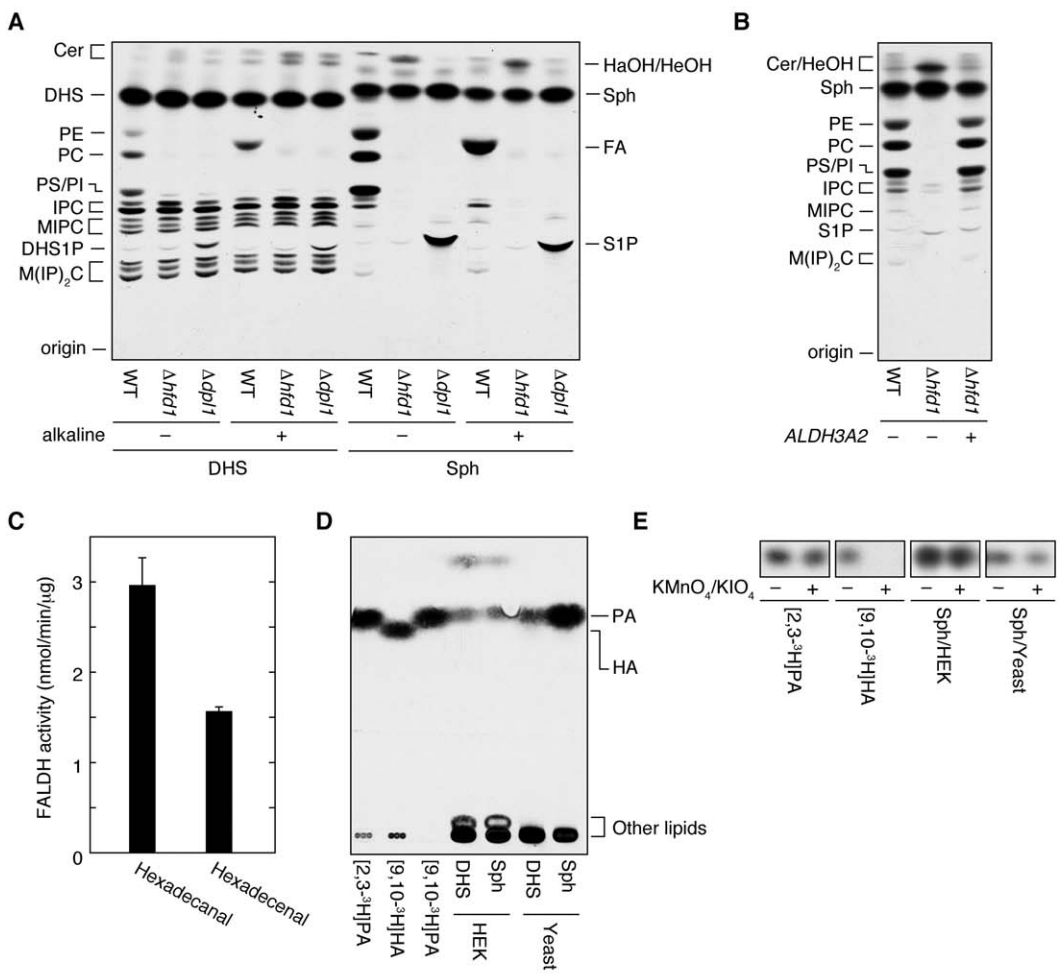
A
Cer
DHS
PE
PC
PS/PI
IPC
MIPC
DHS1P
M(IP)2C
origin
HaOH/HeOH
Sph
FA
S1P
WT
Δhfd1
Δdpl1
alkaline
DHS
Sph
B
Cer/HeOH
Sph
PE
PC
PS/PI
IPC
MIPC
S1P
M(IP)2C
origin
ALDH3A2
C
FALDH activity (nmol/min/μg)
Hexadecanal
Hexadecenal
D
PA
HA
Other lipids
[2,3-3H]PA
[9,10-3H]HA
DHS
Sph
HEK
Yeast
E
KMnO4/KIO4
[2,3-3H]PA
[9,10-3H]HA
Sph/HEK
Sph/Yeast

Fig. 4

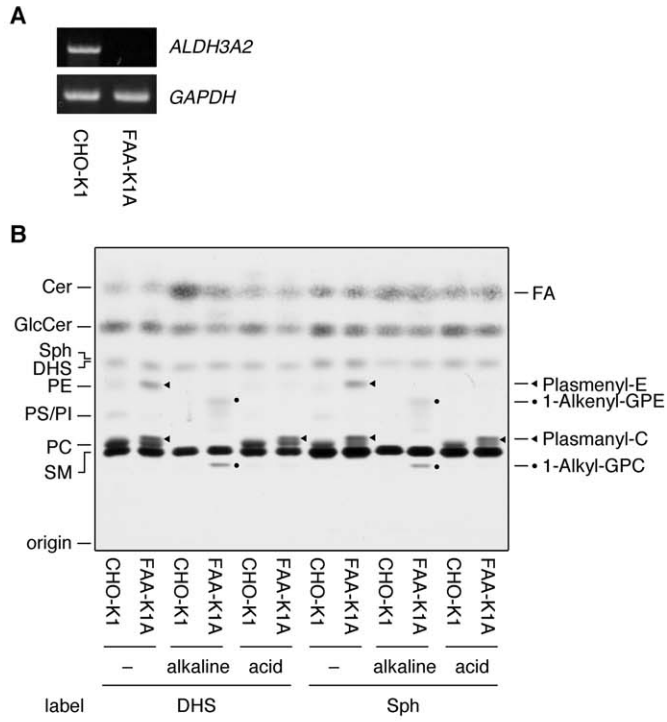
A
ALDH3A2
GAPDH
CHO-K1
FAA-K1A
B
Cer
GlcCer
Sph
DHS
PE
PS/PI
PC
SM
origin
FA
Plasmenyl-E
1-Alkenyl-GPE
Plasmanyl-C
1-Alkyl-GPC
CHO-K1
FAA-K1A
–
alkaline
acid
label
DHS
Sph

Fig. 5

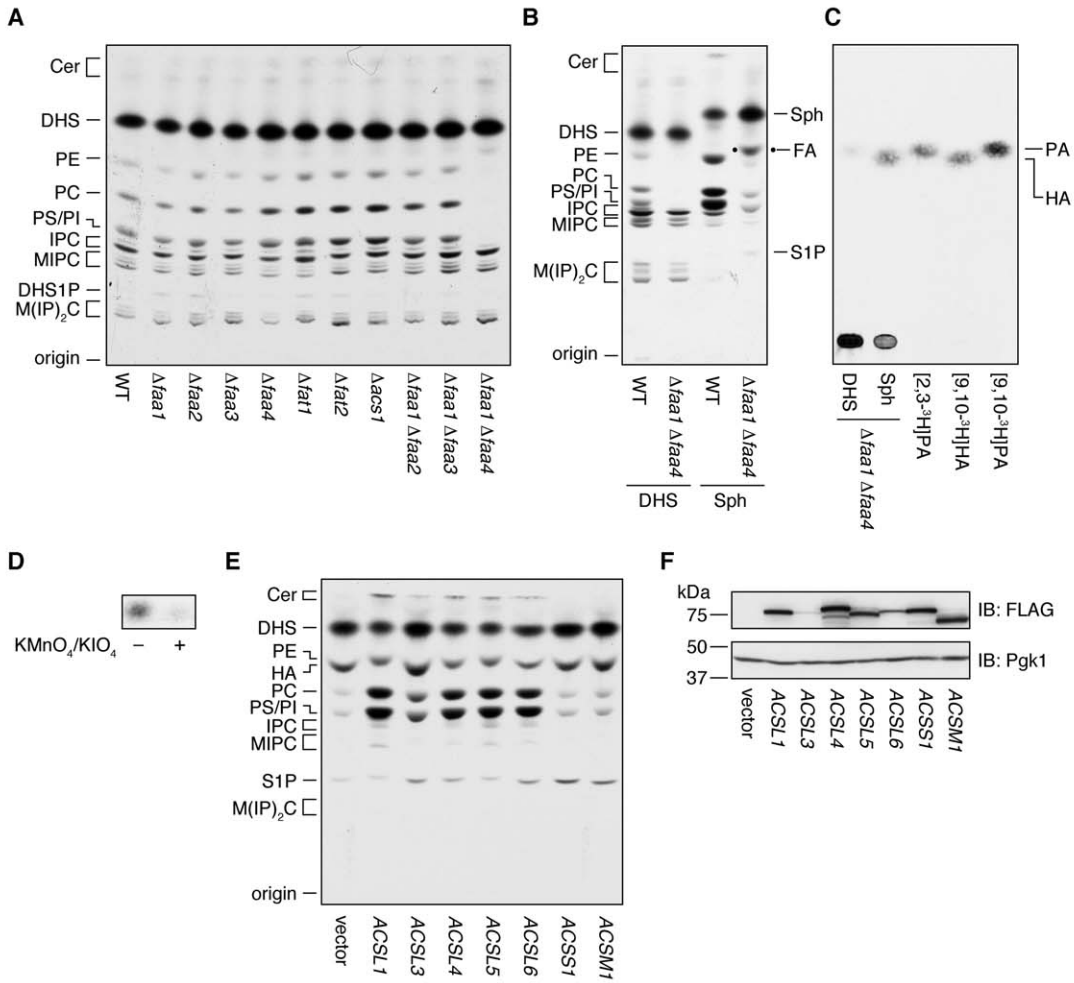
A
Cer
DHS
PE
PC
PS/PI
IPC
MIPC
DHS1P
M(IP)2C
origin
WT
Δfaa1
Δfaa2
Δfaa3
Δfaa4
Δfat1
Δfat2
Δacs1
Δfaa1 Δfaa2
Δfaa1 Δfaa3
Δfaa1 Δfaa4
B
Cer
DHS
PE
PC
PS/PI
IPC
MIPC
M(IP)2C
origin
Sph
FA
S1P
WT
Δfaa1 Δfaa4
WT
Δfaa1 Δfaa4
DHS
Sph
C
PA
HA
DHS
Sph
Δfaa1 Δfaa4
[2,3-3H]PA
[9,10-3H]HA
[9,10-3H]PA
D
KMnO4/KIO4
–
+
E
Cer
DHS
PE
HA
PC
PS/PI
IPC
MIPC
S1P
M(IP)2C
origin
vector
ACSL1
ACSL3
ACSL4
ACSL5
ACSL6
ACSS1
ACSM1
F
kDa
75
50
37
IB: FLAG
IB: Pgk1
vector
ACSL1
ACSL3
ACSL4
ACSL5
ACSL6
ACSS1
ACSM1

Fig. 6

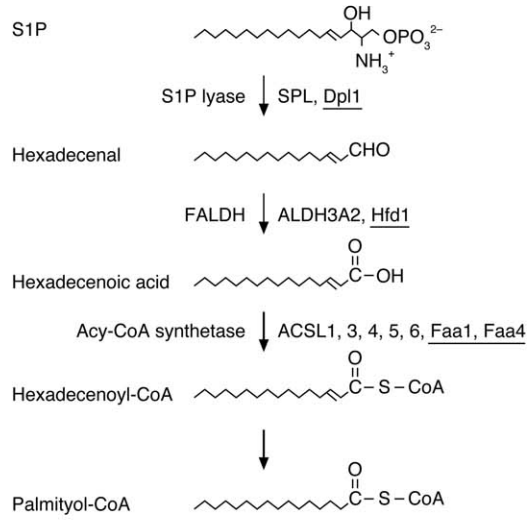
S1P
OH
OPO3 2–
NH3 +
S1P lyase
SPL, Dpl1
Hexadecenal
CHO
FALDH
ALDH3A2, Hfd1
Hexadecenoic acid
O
C–OH
Acy-CoA synthetase
ACSL1, 3, 4, 5, 6, Faa1, Faa4
Hexadecenoyl-CoA
C–S–CoA
Palmityol-CoA

Fig. 7